ELSEVIER

www.elsevier.nl/locate/jorganchem

Journal of Organometallic Chemistry 592 (1999) 103–108

Journal of Organometallic Chemistry

Synthesis and characterization of photosensitive, dinuclear palladium(I) complexes with 1,1′-bis(diphenylphosphino)ferrocene (dppf), $[Pd_2(dppf)_2(RNC)_2]^{2+}$ (R = xylyl and mesityl)

Tomoaki Tanase [a,*], Junko Matsuo [a], Tomoko Onaka [a], Rowshan Ara Begum [a], Makiko Hamaguchi [a], Shigenobu Yano [a], Yasuhiro Yamamoto [b]

[a] *Department of Chemistry, Faculty of Science, Nara Women's University, Kitauoya-higashi-machi, Nara 630-8285, Japan*
[b] *Department of Chemistry, Faculty of Science, Toho University, Miyama 2-2-1, Funabashi, Chiba 274-8510, Japan*

Accepted in revised form 11 August 1999

Abstract

Reactions of the dinuclear palladium(I) complex, $[Pd_2(RNC)_6](PF_6)_2$ (R = 2,6-xylyl (Xyl), 2,4,6-mesityl (Mes)), with 1,1′-bis-(diphenylphosphino)ferrocene (dppf) gave dipalladium(I) complexes with dppf ligands, $[Pd_2(dppf)_2(RNC)_2](PF_6)_2$ (**1**, R = Xyl, 66%; **2**, R = Mes, 18%), which were characterized by elemental analysis, ^{1}H- and ^{31}P-NMR spectroscopy, IR and UV–vis absorption spectroscopic analyses, and cyclic voltammetry. The structure of **1** was characterized by X-ray crystallography. The cation of compound **1** is composed of two Pd(I) atoms joined by a Pd–Pd σ-bond (2.602(1) Å), and each palladium ion has a square planar structure ligated by a terminal isocyanide, two P atoms of dppf, and the neighboring Pd atom. The dppf ligands chelate to the metal with an average P–Pd–P bite angle of 99.19° and an average Pd···Fe distance of 4.236 Å. The cyclopentadienyl rings of dppf ligands are in staggered form. The ^{1}H- and ^{31}P-NMR and the electronic absorption spectra of **1** and **2** indicated that the metal–metal bonded structure as observed in the crystal of **1** was retained in the solution. Complexes **1** and **2** were extremely photosensitive, and underwent a homolytic cleavage even under a room light. The reaction was monitored by the electronic absorption spectral changes and might generate a cation radical, $[Pd(dppf)(RNC)]^+$. The cyclic voltammograms of **1** and **2** in acetonitrile solution showed two successive *quasi*-reversible oxidation waves at $E_{1/2} = 0.60$, 0.72 V (vs. $Ag/AgPF_6$) (**1**) and 0.62, 0.73 V (**2**) and an irreversible reduction wave at $E_{1/2} = -1.23$ V (**1**) and -1.22 V (**2**). The former oxidation waves can be assigned to Fe(II)/Fe(III) processes of the two ferrocenyl groups and demonstrated that a charge-transfer communication between the Fe centers occurred through the Pd–Pd single bond.

Keywords: Palladium; 1,1′-Bis(diphenylphosphino)ferrocene (dppf); Metal–metal bond; Isocyanide; CV

1. Introduction

Metal–metal bonded di- and polynuclear complexes have been of general interest in relevance to photo- and electrochemical materials as well as multimetallic reaction sites. We have systematically studied di-, tri-, and multinuclear complexes of palladium and platinum with isocyanide and diphosphine ligands by the use of chemical and electrochemical procedures [1–10]. Diphosphines, $Ph_2P(CH_2)_nPPh_2$ ($n = 1$–6), *cis*-$Ph_2PCH{=}CHPPh_2$, and $^tBu_2PCH_2CH_2P^tBu_2$, N-based ligands, such as py, bpy, phen, and 2,9-dimethyl phen, and phenyl-substituted cyclopentadienyl groups, $Ph_4C_5H^-$ and $Ph_5C_5^-$, have been introduced into the dipalladium(I) and diplatinum(I) cores ligated by isocyanides to modify reactivities and physical properties of the clusters. In the present study, we have used the diphosphine ligand having ferrocenyl unit, 1,1′-bis(diphenylphosphino)-ferrocene (dppf), as an auxiliary ligand to metal–metal bond. Transition metal complexes with dppf ligand have extensively been studied in homogeneous catalytic reactions and they have also attracted extensive attention in material science, because of their involvement of electrochemically active ferrocenyl unit [11]. Metal–metal bonded dinuclear complexes with dppf ligands could be of potential interest as most

* Corresponding author. Fax: +81-742-203399.

0022-328X/99/$ - see front matter
PII: S0022-328X(99)00496-9

simple multifunctional material including photochemically active metal–metal bond and electrochemically active ferrocenyl unit. In this report, we have prepared metal–metal bonded dipalladium(I) complexes with dppf ligands, $[Pd_2(dppf)_2(RNC)_2](PF_6)$ (R = 2,6-xylyl (Xyl) (**1**) and 2,4,6-mesityl (Mes) (**2**)), which were proved to be extremely photosensitive and showed an interesting charge-transfer-communication through the Pd–Pd bond.

2. Experimental

2.1. Materials

Dichloromethane and acetonitrile were distilled over calcium hydride and benzene and diethyl ether over lithium aluminum hydride prior to use. Other reagents were of the best commercial grade and were used as received. $[Pd_2(RNC)_4Cl_2]$ and $[Pd_2(RNC)_6](PF_6)_2$ [12–14], and 1,1′-bis(diphenylphosphino)ferrocene (dppf)[15] were prepared by the known methods. All reactions were carried out under a nitrogen atmosphere with standard Schlenk and vacuum-line techniques.

2.2. Measurements

^{1}H-NMR spectra were measured on a Varian Gemini 2000 instrument at 300 MHz. Chemical shifts were calibrated to tetramethylsilane as an external reference. $^{31}P\{^1H\}$-NMR spectra were recorded by the same instruments at 121 MHz with chemical shifts being referenced to 85% H_3PO_4 as an external standard. Infrared absorption spectra were recorded with Jasco FT/IR-430 by using Nujol mull, and UV–vis absorption spectra were measured on a Shimazu UV3000 spectrophotometer. Cyclic voltammograms were measured with a BASCV-50W Voltammetric Analyzer by using a conventional three electrode system, glassy carbon (working electrode), platinum wire (counter electrode), and $Ag/AgPF_6$ (in CH_3CN) reference electrode.

2.3. Preparation of $[Pd_2(dppf)_2(RNC)_2](PF_6)_2$ (R = Xyl (**1**), Mes (**2**))

2.3.1. Method A

The diphosphine dppf (98 mg, 0.18 mmol) was added to a dichloromethane solution (10 ml) of $[Pd_2(XylNC)_6](PF_6)_2$ (113 mg, 0.088 mmol). The mixture was stirred at room temperature (r.t.) for 12 h, and the solvent was removed under reduced pressure. The residue was washed with diethyl ether (2 × 10 ml) and was extracted with 20 ml of dichloromethane. The extract, after passing through a glass filter, was concentrated to ca. 5 ml. Benzene was slowly added to the solution to give dark red crystals of $[Pd_2(dppf)_2(XylNC)_2](PF_6)_2\cdot 2.5CH_2Cl_2$ (**1**·2.5CH_2Cl_2) in 66% yield, which were washed with Et_2O and dried in vacuo. Anal. Calc. for $C_{88.5}H_{79}N_2P_6F_{12}Pd_2Cl_5$: C, 50.95; H, 3.82; N, 1.34%. Found: C, 50.85 H, 3.98; N, 1.62%. IR (Nujol): 2142 (s), 1482, 1437, 1400, 1305, 1168, 1096, 1032, 998, 843 (s), 783 cm^{-1}. ^{1}H-NMR (CD_2Cl_2): δ 1.71 (s, *o*-Me, 12H), 3.00 (br, Cp, 4H), 4.04 (s, Cp, 2H), 4.08 (s, Cp, 2H), 4.12 (s, Cp, 2H), 4.24 (s, Cp, 2H), 4.36 (s, Cp, 2H), 4.71 (s, Cp, 2H), 6.7–7.9 (m, Ar, 46H). $^{31}P\{^1H\}$-NMR (CD_2Cl_2): δ 6.57, 24.77 (d, $J_{PP'} = 6.1$ Hz). UV-vis (in CH_2Cl_2): λ (log ε) 449 (4.23), 532sh (3.83) nm (M^{-1} cm^{-1}). Similar procedures using $[Pd_2(MesNC)_6](PF_6)_2$ gave dark red crystals of $[Pd_2(dppf)_2(MesNC)_2](PF_6)_2\cdot 0.5CH_2Cl_2$ (**2**·0.5CH_2Cl_2) in 18% yield. Anal. Calc. for $C_{88.5}H_{79}N_2P_6F_{12}Pd_2Cl$: C, 54.67; H, 4.10; N, 1.44%. Found: C, 54.34 H, 4.31; N, 1.52%. IR (Nujol): 2142 (s), 1482, 1437, 1313, 1167, 1096, 1034, 1000, 840 (s), 745, 698 cm^{-1}. ^{1}H-NMR (CD_2Cl_2): δ 1.64 (s, *o*-Me, 12H), 2.33 (s, *p*-Me, 6H), 2.98(br, Cp, 4H), 4.02 (s, Cp, 2H), 4.05 (s, Cp, 2H), 4.09 (s, Cp, 2H), 4.22 (s, Cp, 2H), 4.34 (s, Cp, 2H), 4.68 (s, Cp, 2H), 6.7–7.9 (m, Ar, 44H). $^{31}P\{^1H\}$-NMR (CD_2Cl_2): δ 6.28, 24.62 (d, $J_{PP'} = 5.5$ Hz). UV-vis (in CH_2Cl_2): λ (log ε) 449 (4.26), 532sh (3.88) nm (M^{-1} cm^{-1}).

2.3.2. Method B

To a dichloromethane (8 ml)–acetone (8 ml) mixed solvent containing $[Pd_2(RNC)_4Cl_2]$ (0.12 mmol) was added dppf (0.25 mmol). The solution was stirred at r.t. for 2.5 h and NH_4PF_6 (0.66 mmol) was added to the solution. The reaction mixture was further stirred at r.t. for 12 h, and then, the solvent was removed under reduced pressure. The residue was washed with Et_2O (2 × 10 ml) and was extracted with 20 ml of dichloromethane. The extract was passed through a glass filter to remove inorganic salts and concentrated to ca. 7 ml. Small portion of benzene was slowly added to the solution to afford dark red crystals of **1**·2.5CH_2Cl_2 (R = Xyl, 34%) and **2**·0.5CH_2Cl_2 (R = Mes, 19%).

2.4. X-ray crystallographic analysis of $[Pd_2(dppf)_2(XylNC)_2](PF_6)_2\cdot 3CH_2Cl_2\cdot C_6H_6$ (**1**·3CH_2Cl_2·C_6H_6)

The crystal of **1**·3CH_2Cl_2·C_6H_6 used in data collection was mounted on the top of a glass fiber with Paraton N oil at −118°C. Crystal data and experimental conditions are summarized in Table 1. All data were collected on a Rigaku AFC7R diffractometer equipped with graphite monochromated Mo–K_α ($\lambda = 0.71069$ Å) radiation. The cell constants were obtained from least-square refinements of 20 reflections with $20 < 2\theta < 30°$. Three standard reflections were monitored every 150 reflections and showed no systematic decrease in inten-

Table 1
Crystallographic and experimental data for $[Pd_2(dppf)_2(XylNC)_2](PF_6)_2 \cdot 3CH_2Cl_2 \cdot C_6H_6$ (**1**·$3CH_2Cl_2 \cdot C_6H_6$)

Empirical formula	$C_{95}H_{86}N_2P_6F_{12}Cl_6Fe_2Pd_2$
Formula weight	2206.77
Crystal system	Monoclinic
Space group	$P2_1/c$ (no. 14)
a (Å)	20.946(7)
b (Å)	14.578(5)
c (Å)	30.233(9)
β (°)	96.17(3)
V (Å^3)	9178(4)
Z	4
T (°C)	−118
$D_{calc.}$ (g cm^{-1})	1.597
Absorption coefficient (cm^{-1})	10.47
Transmission factor	0.97–0.99
2θ range (°)	$3 \leq 2\theta \leq 45$
h, k, l range	$+h$, $+k$, $\pm l$
Scan method	$\omega - 2\theta$
Scan speed (° min^{-1})	16
No. of unique data	12635
No. of observed data	6557 ($I \geq 3\sigma(I)$)
No. of variables	771
R [a]	0.059
R_w [b]	0.064
Goodness-of-fit [c]	1.49

[a] $R = \Sigma||F_o| - |F_c||/\Sigma|F_o|$.
[b] $R_w = [\Sigma\, w(|F_o| - |F_c|)^2/\Sigma\, w|F_o|^2]^{1/2}$ ($w = 1/\sigma^2(F_o)$).
[c] Goodness-of-fit $= [\Sigma\, w(|F_o| - |F_c|)^2/(N_o - N_p)]^{1/2}$ (N_o = no. of data, N_p = no. of variables).

sity. Reflection data were corrected for Lorentz-polarization and absorption effects (ψ-scan method).

The structure of **1** was solved by direct methods with SIR92 [16]. The two palladium atoms and the most non-hydrogen atoms were located initially and subsequent different Fourier syntheses gave the positions of other non-hydrogen atoms. The coordinates of all hydrogen atoms were calculated at ideal positions with the C–H distance of 0.95 Å. The structure was refined with the full-matrix least-square techniques on F minimizing $\Sigma\, w(|F_o| - |F_c|)^2$. Final refinement with isotropic temperature factors for the carbon atoms of phenyl and xylyl groups and solvent molecules and with anisotropic thermal parameters for the other non-hydrogen atoms converged to $R = 0.059$ and $R_w = 0.064$, where $R = \Sigma||F_o| - |F_c||/\Sigma|F_o|$ and $R_w = [\Sigma\, w(|F_o| - |F_c|)^2/\Sigma\, w|F_o|^2]^{1/2}$ ($w = 1/\sigma^2(F_o)$). One dichloromethane solvent molecule disordered and was refined with three Cl atoms with 1.0, 0.5, and 0.5 occupancies. Atomic scattering factors and values of f' and f'' for Pd, Cl, P, F, N, and C were taken from the literature [17]. All calculations were carried out on a Silicon Graphics O2 Station with the TEXSAN Program System [18]. The perspective views were drawn by using the program ORTEP-II [19].

3. Results and discussion

3.1. Preparation and characterization of $[Pd_2(dppf)_2(RNC)_2](PF_6)_2$

Reaction of $[Pd_2(RNC)_6](PF_6)_2$ with two equivalents of dppf in dichloromethane yielded dark red dipalladium(I) complexes, $[Pd_2(dppf)_2(RNC)_2](PF_6)_2$ (R = Xyl (**1**), Mes (**2**)). Complexes **1** and **2** could also be obtained by the reaction of $[Pd_2(RNC)_4Cl_2]$ with dppf and NH_4PF_6. Elemental analyses are consistent with the formula, and the IR spectra showed bands corresponding to the N≡C stretching of terminal isocyanides at 2142 cm^{-1}. The ^{1}H-NMR spectra indicated the presence of isocyanide and 1,1′-bis(diphenylphosphino)-ferrocene in a 1:1 ratio (Fig. 1(a)). The *o*-methyl protons of isocyanide ligands were observed as a singlet

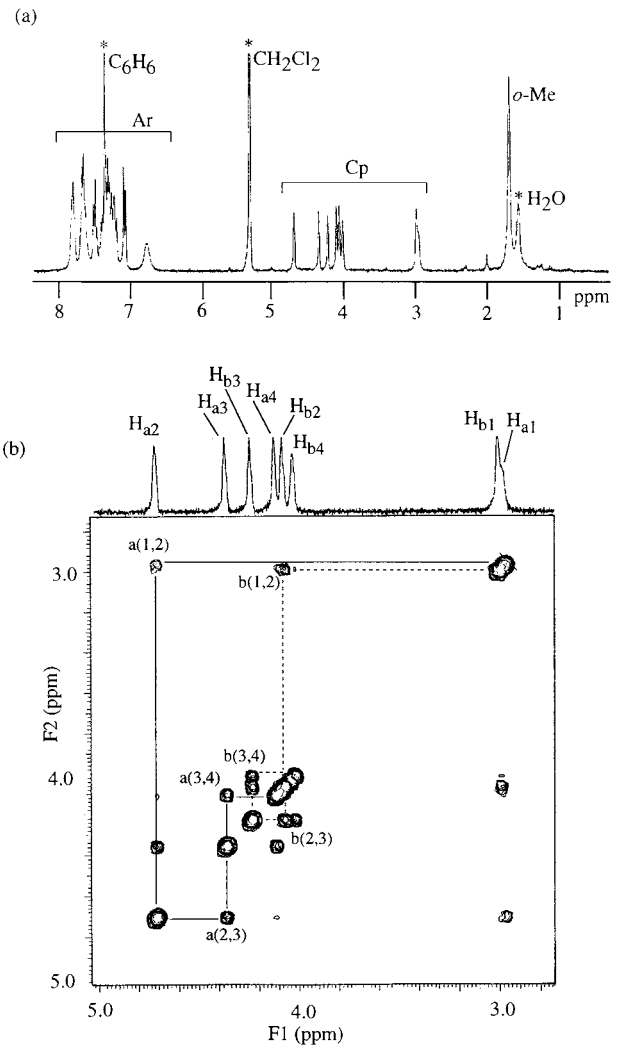

Fig. 1. (a) ^{1}H-NMR spectrum of $[Pd_2(dppf)_2(XylNC)_2](PF_6)_2$ (**1**) in CD_2Cl_2. Asterisks correspond to solvent peaks involve in the complex and impurity. (b) ^{1}H-^{1}H COSY spectrum in CD_2Cl_2 in the region of cyclopentadienyl protons.

at δ 1.71 and resonances for two sets of cyclopentadienyl groups were observed at δ 3.00–4.71, which were assigned by ^{1}H-^{1}H COSY spectrum to two spin sequences H_{a1-4} and H_{b1-4} (Fig. 1(b)). In the $^{31}P\{^1H\}$-NMR spectra, two doublets were observed at δ 6.57 and 24.77 with $J_{PP'} = 6.1$ Hz (**1**) and δ 6.28 and 24.62 with $J_{PP'} = 5.5$ Hz (**2**). These spectral patterns are indicative of nonequivalent two *cis*-P atoms of dppf ligands chelating to the Pd center. The electronic absorption spectra in dichloromethane showed a band at 449 nm, characteristic of Pd(I)–Pd(I) core, and broad shoulder feature in the lower energy side around 536 nm (Fig. 2). The latter shoulder band was not observed for dppf and for dipalladium(I) dimers with diphosphines ($Ph_2P(CH_2)_nPPh_2$, $n = 2$–4). The dark-colored complexes **1** and **2** were extremely photosensitive and were readily decomposed in dichloromethane, acetone, or acetonitrile solution even under room light, which could be monitored by the electronic absorption spectral changes (Fig. 3). Complexes **1** and **2** were stable in the solutions under dark. The characteristic absorption around 449 nm, assignable to the $\sigma \rightarrow \sigma^*$ transition of the Pd–Pd bond, decreased and finally no appreciable absorption was observed in the region $\lambda > 400$ nm. These spectral changes indicated that a photo-induced Pd–Pd bond breaking took place to generate a cation radical species, $[Pd(I)(dppf)(XylNC)]^+$, which could be further quenched by solvents to stable Pd(II) complexes, although they were not isolated and characterized.

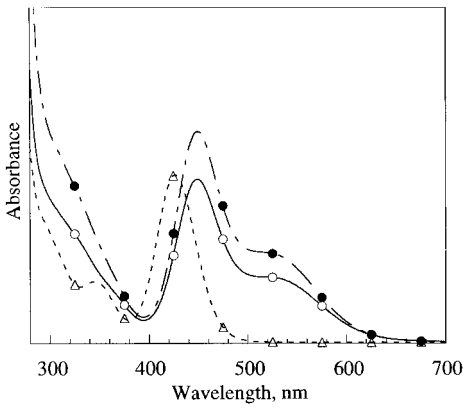

Fig. 2. UV–vis absorption spectra of (a) $[Pd_2(dppf)_2(XylNC)_2](PF_6)_2$ (**1**) (○); (b) $[Pd_2(dppf)_2(MesNC)_2](PF_6)_2$ (**2**) (●); and (c) $[Pd_2(dppp)_2(MesNC)_2](PF_6)_2$ (**3**) (△) in dichloromethane.

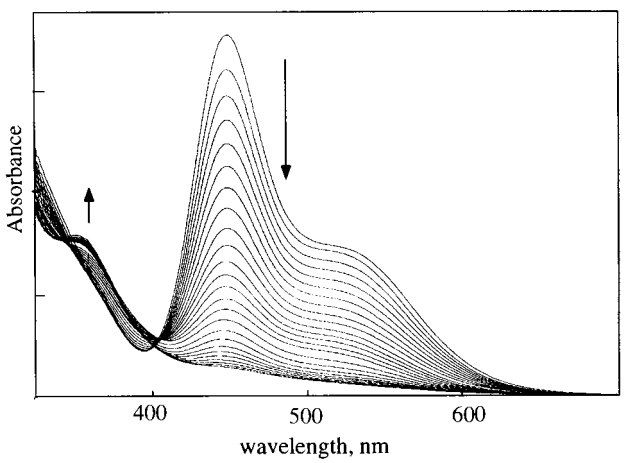

Fig. 3. UV–vis spectral changes of $[Pd_2(dppf)_2(XylNC)_2](PF_6)_2$ (**1**) in acetone under room right. Monitored every 30 min.

3.2. Crystal structure of $[Pd_2(dppf)_2(XylNC)_2](PF_6)_2$ (*1*)

The structure of complex **1** in the solid state was determined by X-ray crystallography. The asymmetric unit contains a complex cation, two hexafluorophosphate anions, three dichloromethane and one benzene molecules without unusual contacts between them. A perspective view of the complex cation of **1** is illustrated in Fig. 4, and some selected bond lengths and angles are listed in Table 2. The complex cation consists of two palladium atoms joined by a Pd–Pd σ-bond. The

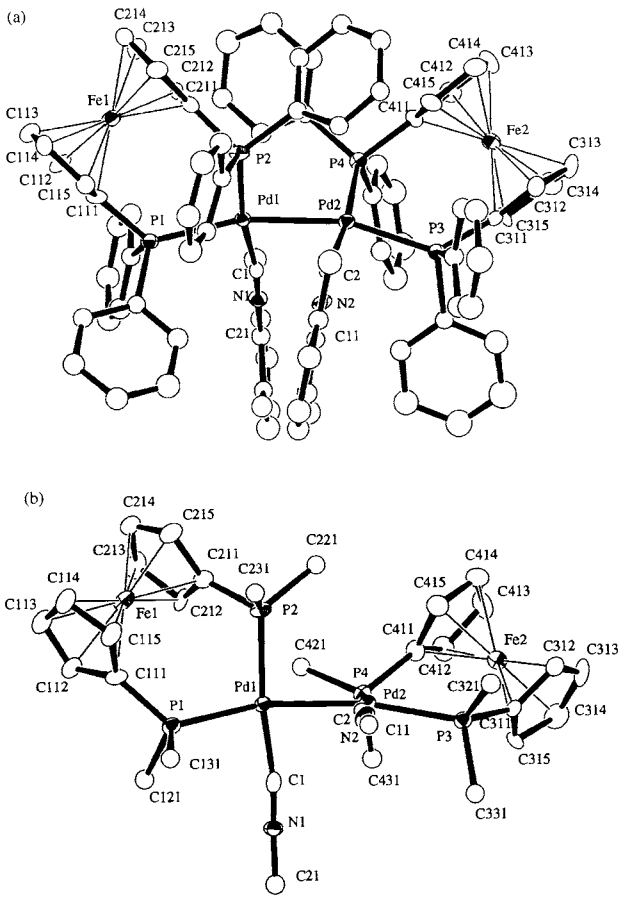

Fig. 4. (a) ORTEP diagram for the complex cation of $[Pd_2(dppf)_2(XylNC)_2](PF_6)_2$ (**1**). Hydrogen atoms are omitted for clarity. (b) ORTEP view of the complex cation with phenyl rings of dppf and xylyl rings of XylNC being omitted for clarity.

Table 2
Selected bond distances (Å) and angles (°) for $\mathbf{1}\cdot 3CH_2Cl_2\cdot C_6H_6$ [a]

Bond distances			
Pd(1)–Pd(2)	2.602(1)	Pd(1)–P(1)	2.385(3)
Pd(1)–P(2)	2.326(3)	Pd(1)–C(1)	2.01(1)
Pd(2)–P(3)	2.380(3)	Pd(2)–P(4)	2.341(3)
Pd(2)–C(2)	1.986(9)	Fe(1)–C(111)	2.029(9)
Fe(1)–C(112)	2.06(1)	Fe(1)–C(113)	2.06(1)
Fe(1)–C(114)	2.04(1)	Fe(1)–C(115)	2.03(1)
Fe(1)–C(211)	2.02(1)	Fe(1)–C(212)	2.027(9)
Fe(1)–C(213)	2.08(1)	Fe(1)–C(214)	2.05(1)
Fe(1)–C(215)	2.00(1)	Fe(2)–C(311)	2.016(9)
Fe(2)–C(312)	2.05(1)	Fe(2)–(313)	2.08(1)
Fe(2)–C(314)	2.04(1)	Fe(2)–C(315)	2.04(1)
Fe(2)–C(411)	2.01(1)	Fe(2)–C(412)	2.04(1)
Fe(2)–C(413)	2.05(1)	Fe(2)–C(414)	2.06(1)
Fe(2)–C(415)	2.00(1)	N(1)–C(1)	1.14(1)
N(1)–C(11)	1.39(1)	N(2)–C(2)	1.16(1)
N(2)–C(21)	1.41(1)		
Bond angles			
Pd(2)–Pd(1)–P(1)	165.30(7)	Pd(2)–Pd(1)–P(2)	92.60(8)
Pd(2)–Pd(1)–C(1)	79.6(3)	P(1)–Pd(1)–P(2)	98.5(1)
P(1)–Pd(1)–C(1)	90.1(3)	P(2)–Pd(1)–C(1)	170.4(3)
Pd(1)–Pd(2)–P(3)	162.21(7)	Pd(1)–Pd(2)–P(4)	95.72(7)
Pd(1)–Pd(2)–C(2)	77.0(3)	P(3)–Pd(2)–P(4)	99.84(9)
P(3)–Pd(2)–C(2)	87.5(3)	P(4)–Pd(2)–C(2)	172.7(3)
C(1)–N(1)–C(21)	174.7(9)	C(2)–N(2)–C(11)	179.3(9)
Pd(1)–C(1)–N(1)	172.0(9)	Pd(2)–C(2)–N(2)	171.2(9)

[a] Estimated standard deviations are given in parentheses.

structure has a *pseudo* C_2 symmetry and is similar to those of $[Pd_2(dppp)_2(MesNC)_2]^{2+}$ (**3**) and $[Pd_2(dppen)_2(XylNC)_2]^{2+}$ (**4**) [5]. Each Pd atom is ligated by two phosphorous atoms of bidentate dppf ligand, a terminal carbon atom of XylNC, and another Pd atom in a planar array. The Pd–Pd bond is not supported by any bridging ligands. The Pd–Pd bond length of 2.602(1) Å is longer than those found in dipalladium(I)–isocyanide complexes without phosphine ligands, $[Pd_2(MeNC)_6](PF_6)_2$ (**5**, 2.531(1) Å) [20–22], $[Pd_2Cl_2(^tBuNC)_4]$ (**6**, 2.532(2) Å) [14], and $[Pd_2I_2(MeNC)_4]$ (**7**, 2.533(1) Å).[23] and comparable to those in the dimers with chelating diphosphines, **3** (2.617(2) Å) and **4** (2.602(1) Å). The dihedral angle between the two $[PdP_2C]$ coordination planes is 89.5°, nearly perpendicular as observed in **3** (86°), **4** (78°), **5** (86.4°) [20–22], **6** (82.7°) [14], and **7** (85.3°) [23]. It is probably due to minimizing the steric repulsion between the bulky isocyanide ligands [5]. The axial P atoms are bending from a colinear arrangement with the Pd–Pd bond, the average Pd–Pd–P_{ax} angle being 163.75°, which could be owing to the steric bulkiness of dppf having the large bite angle of 99.8°. The averages of the Pd–C–N and C–N–C angles are 171.6 and 177.0 °, respectively, which fall within the usual range for terminal isocyanides. The isocyanide ligands are bent toward the Pd–Pd bond, the average Pd–Pd–C angle being 78.3°. The similar inward bend has also been observed in **3**–**7** and other Pd(I) dimers with isocyanide ligands.

Each dppf ligand chelates to the Pd center in a usual manner. The Pd–Fe interatomic distances are 4.223(2) Å (Pd(1)···Fe(1)) and 4.248(2) Å (Pd(2)···Fe(2)), indicating no bonding interaction between the Pd and Fe centers. The two cyclopentadienyl rings of dppf ligands are almost parallel with the dihedral angles of 2.0 and 2.5° and are in staggered arrangement to each other with the average twist angles of 31 and 34°. The Fe–C bond lengths are ranging from 2.01(1) to 2.08(1) Å, exhibiting a normal η^5-fashion of the Cp rings.

On the basis of Cambridge Crystallographic Data analysis, the present complex **1** is the first example of structurally characterized metal–metal bonded dipalladium(I) complex involving ferrocenyl units, although a couple of dipalladium(II) complexes of dppf without metal–metal bond, $[Pd(II)_2(\mu\text{-}Cl)_2(dppf)_2](PF_6)_2$ [24], and $[Pd(II)_2Ag_2Cl_2(\mu\text{-}S)_2(dppf)_2]$ [25], and $[\{Pd(II)_2(\mu\text{-}I)_2I_2\}\{Os_2(\mu\text{-}I)_2I_2(CO)_4\}(dppf)_2]$ [26], have been reported thus far. Further, complex $[Pt_2(\mu\text{-}H)(\mu\text{-}CO)(dppf)_2](BF_4)$ [27] has been characterized as a sole example of metal–metal bonded diplatinum(I) complex.

3.3. Electrochemical property

The cyclic voltammograms (CVs) of complexes **1** and **2** in acetonitrile solution were measured with a glassy carbon working electrode (Fig. 5). The CVs of **1** and **2** showed an irreversible reduction wave at $E^3_{pc} = -1.23$ V (**1**) and -1.22 V (**2**) (vs. $Ag/AgPF_6$) and two-step *quasi* reversible oxidation processes at $E^1_{1/2} = 0.60$ V and $E^2_{1/2} = 0.72$ V for **1** and $E^1_{1/2} = 0.62$ V and $E^2_{1/2} = 0.73$ V for **2** with peak-to-peak separations, $E^i_{pa} - E^i_{pc}$, of 60–70 mV. In the light of electrochemical data for the metal–metal bonded dipalladium(I) complexes with

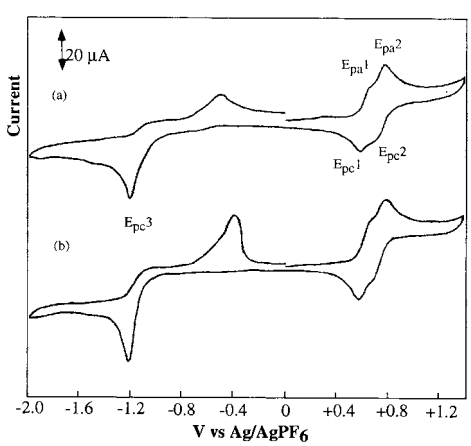

Fig. 5. Cyclic voltammograms of (a) $[Pd_2(dppf)_2(XylNC)_2](PF_6)_2$ (**1**) and (b) $[Pd_2(dppf)_2(MesNC)_2](PF_6)_2$ (**2**) in acetonitrile (1 mM) involving $[nBu_4N][PF_6]$ (0.1 M) as supporting electrolyte, measured with a glassy carbon working electrode with a scan rate of 100 mV s^{-1}.

diphosphine ligands, $[Pd_2(diphos)_2(RNC)_2](PF_6)_2$ (diphos = dppe, dppp, dppen), the irreversible reduction wave corresponds to a Pd(I) → Pd(0) reduction process occurring simultaneously on both Pd centers [5]. The reduction potential is notably higher than that of the analogous compounds, $[Pd_2(dppp)_2(MesNC)_2](PF_6)_2$ (−1.45 V). The latter *quasi*-reversible oxidation waves can be assigned to two-step one-electron oxidations of the ferrocenyl groups, in the light of CV data for the mononuclear Pd complex with dppf [28,29]. The potential separation, $\Delta E_{1/2} = E^2_{1/2} - E^1_{1/2}$, of 120 mV (**1**) and 110 mV (**2**) indicated that a charge-transfer communication between the two ferrocenyl centers occurred presumably through the Pd–Pd single bond. Namely, stepwise one-electron redox processes, $[Fe^{II}Pd^{I}Pd^{I}Fe^{II}] \leftrightarrow [Fe^{III}Pd^{I}Pd^{I}Fe^{II}] \leftrightarrow [Fe^{III}Pd^{I}Pd^{I}Fe^{III}]$, could be envisaged from the cyclic voltammograms. Conproportionation constant K_c, defined by $[Fe^{II}Pd^{I}Pd^{I}Fe^{II}] + [Fe^{III}Pd^{I}Pd^{I}Fe^{III}] \leftrightarrow 2[Fe^{III}Pd^{I}Pd^{I}Fe^{II}]$, is useful to evaluate the stability of the $Fe^{III}Pd^{I}Pd^{I}Fe^{II}$ mixed-valence species, and is calculated by using the equation $K_c = \exp[(E^2_{1/2} - E^1_{1/2})n_1n_2F/RT]$, where F is the Faraday constant and n_i is the number of electrons in step i.[30] The K_c values are estimated to be ca. $1.1–0.7 \times 10^2$ in the present cases. Richardson and Taube also reported that when $\Delta E_{1/2}$ is less than 150 mV, the two-step waves in the CV are not resolved and, in such cases, $E_p - E_{p/2}$ values could be used to determine $\Delta E_{1/2}$, where $E_{p/2}$ is the potential at which the current is half the peak current at E_p [30]. On the basis of their tabulations of $\Delta E_{1/2}$ versus $E_p - E_{p/2}$, the K_c value was calculated as 1.1×10^2 ($E_{pa} - E_{pa/2} = 150$ mV, $\Delta E_{1/2} = 120$ mV for **1** and **2**).

4. Conclusions

The highly photosensitive Pd_2Fe_2 mixed metal complexes, $[Pd_2(dppf)_2(RNC)_2](PF_6)_2$ (R = Xyl, Mes), were successfully prepared and characterized. They also showed an interesting charge-transfer communication between the two Fe centers through the Pd–Pd single bond.

5. Supplementary material

Tables of experimental conditions, complete atomic positional parameters, anisotropic temperature factors, and bond distances and angles for $\mathbf{1}\cdot 3CH_2Cl_2\cdot C_6H_6$, and a listing of observed and calculated structure factors are available from the author (T.T.) on request.

Acknowledgements

This work was partly supported by Grants-in-Aid from the Ministry of Education, Science, Culture, and Sports, Japan.

References

[1] Y. Yamamoto, K. Takahashi, H. Yamazaki, J. Am. Chem. Soc. 108 (1986) 2458.
[2] T. Tanase, Y. Kudo, M. Ohno, K. Kobayashi, Y. Yamamoto, Nature 344 (1990) 526.
[3] T. Tanase, T. Horiuchi, Y. Yamamoto, K. Kobayashi, J. Organomet. Chem. 440 (1992) 1.
[4] Y. Yamamoto, H. Yamazaki, Organometallics 12 (1993) 933.
[5] T. Tanase, K. Kawahara, H. Ukaji, K. Kobayashi, H. Yamazaki, Y. Yamamoto, Inorg. Chem. 32 (1993) 3682.
[6] T. Tanase, H. Ukaji, Y. Kudo, M. Ohno, K. Kobayashi, Y. Yamamoto, Organometallics 13 (1994) 1374.
[7] Y. Yamamoto, H. Yamazaki, Inorg. Chem. 25 (1986) 3327.
[8] T. Tanase, T. Nomura, Y. Yamamoto, K. Kobayashi, J. Organomet. Chem. 410 (1991) C25.
[9] T. Tanase, T. Nomura, T. Fukushima, Y. Yamamoto, Inorg. Chem. 32 (1993) 4578.
[10] T. Tanase, T. Fukushima, T. Nomura, Y. Yamamoto, Inorg. Chem. 33 (1994) 32.
[11] A. Togni, T. Hayashi, Ferrocenes — Homogeneous Catalysis, Organic Synthesis, Materials Science, VCH, Weinheim, Germany, 1995.
[12] S. Otsuka, Y. Tatsuno, K. Ataka, J. Am. Chem. Soc. 93 (1971) 6705.
[13] J.R. Boehm, A.L. Balch, Inorg. Chem. 16 (1977) 778.
[14] Y. Yamamoto, H. Yamazaki, Bull. Chem. Soc. Jpn. 58 (1985) 1843.
[15] R.-J. de Lang, J.V. Soolingen, H.D. Verkruijsse, L. Brandsma, Synth. Commun. 25 (1995) 2989.
[16] M.C. Burla, M. Camalli, G. Cascarano, C. Giacovazzo, G. Polidori, R. Spagna, D. Viterbo, J. Appl. Crystallogr. 22 (1989) 389.
[17] (a) D.T. Cromer, J.T. Waber, International Tables for X-ray Crystallography, vol. IV, Kynoch, Birmingham, UK, 1974. (b) D.T. Cromer, Acta Crystallogr. 18 (1965) 17.
[18] TEXSAN Structure Analysis Package, Molecular Structure Corporation, The Woodlands, TX, 1985.
[19] C.K. Johnson, ORTEP-II, Oak Ridge National Laboratory, Oak Ridge, TN, 1976.
[20] D.J. Doonan, A.L. Balch, S.Z. Goldgerg, R. Eisengerg, J.S. Miller, J. Am. Chem. Soc. 97 (1975) 1961.
[21] S.Z. Goldberg, R. Eisenberg, Inorg. Chem. 15 (1976) 535.
[22] T.D. Miller, M.A.S. Clair, M.K. Reinking, C.P. Kubiak, Organometallics 2 (1983) 767.
[23] N.M. Rutherford, M.M. Olmstead, A.L. Balch, Inorg. Chem. 23 (1984) 2833.
[24] Z.-H. Huang, Z.-X. Huang, H.-H. Zhang, J. Struct. Chem. 16 (1997) 324.
[25] G. Li, S. Li, A.L. Tan, W.-H. Yip, T.C.K. Mak, T.S.A. Hor, J. Chem. Soc. Dalton Trans. (1996) 4315.
[26] J.W.-S. Hui, W.-T. Wong, J. Chem. Soc. Dalton Trans. (1997) 2445.
[27] A.L. Bandini, G. Banditelli, M.A. Cinellu, G. Sanna, G. Minghetti, F. Demartin, M. Manassero, Inorg. Chem. 28 (1989) 404.
[28] W.-H. Leung, J.L. Chim, W.-T. Wong, J. Chem. Soc. Dalton Trans. (1997) 3277.
[29] M. Zhou, Y.X.A.-M. Tan, P.-H. Leung, K.F. Mok, L.-L. Koh, T.S.A. Hor, Inorg. Chem. 34 (1995) 6425.
[30] D.E. Richardson, H. Taube, Inorg. Chem. 20 (1981) 1278.